Pak. J. Bot., 49(6): 2285-2293, 2017.

METABOLOMIC DIFFERENTIATION OF *RHODIOLA CRENULATA* FROM DIFFERENT GEOGRAPHICAL ORIGINS OF SICHUAN PROVINCE AND TIBET, CHINA

TAO LI*, XUAN HE AND QIAOQI LUO

Department of Natural Medicine, Sichuan University, West China School of Pharmacy, and Key Laboratory of Drug Targeting, Ministry of Education, No. 17, Section 3, Ren-Min-Nan-Lu Road, Chengdu, Sichuan 610041, P. R. China
**Corresponding author's email: scdxlitao@scu.edu.cn ; Tel. : +86 28 85501146*

Abstract

Rhodiola crenulata (HK.f. et Thoms.) H.Ohba is a popularly used ethnodrug from the Qinghai-Tibetan plateau of China and a range of biological activities have been attributed to it. The chemical composition of *R. crenulata* is highly variable and its quality is often controlled on the basis of one or two marker compounds. In order to find out a suitable method for the quality control of this material, the metabolomic comparative analysis of the methanol extract of the twelve geographical origins of *R. crenulata* was carried out by ^{1}H NMR spectroscopy and multivariate data analysis techniques. Principal component analysis (PCA) and partial least squares (PLS) methods were applied to discriminate the samples of twelve geographical origins. The chemical compositions of the cohort are diverse and mostly mapped and well classified according to geographical origins and the month of collection. A broad range of metabolites were detected by ^{1}H NMR spectroscopy without any chromatographic separation. The principal component analysis and partial least squares methods used to reduce the huge data set obtained from the ^{1}H NMR spectra of the plant extract clearly discriminated various geographical regions of *R. crenulata*. The major differences in various geographical regions of *R. crenulata* were found to be due to phenylpropanoids, flavonoids, terpenes, and carbohydrates.The approach provides useful information and gives an overview of the difference between crude drugs of *R. crenulata* originating from different production environments. This method will be a useful tool for quality evaluation of *R. crenulata* so as to ensure batch-to-batch uniformity for crude drugs, and lay the foundation for the selection of optimal samples of geographical origins and cultivation locality of *R. crenulata* with excellent quality and consequently curative effects according to clinic application.

Key words: NMR spectroscopy; *Rhodiola crenulata*; Metabolic fingerprinting; Phenylpropanoids; Flavonoids; Terpenes; Carbohydrates; Principal component analysis.

Introduction

Rhodiola, known as Hong Jingtian in Chinese, has been used as an important adaptogen, hemostatic, and tonic in traditional Tibetan medicines (TTM) named "Suo-Luo-Ma-Bao" for thousands of years in China (Yang *et al.*, 1991). *Rhodiola* plants are mainly distributed in Tibet and in Sichuan province. Most notably, the roots and rhizomes of *R. crenulata* (HK.f. et Thoms.) H.Ohba are generally regarded as the best quality that have been accepted by the Pharmacopoeia of China (2015) and are used for improving blood circulation, thoracic obstruction, cardiodynia, apoplexy, hemiplegia, lassitude and asthma (Committee of National Pharmacopoeia, 2015).

In both traditional and more recent popular uses, the pharmacological effects are mainly attributed to different classes of compounds (phenylpropanoids, flavonoids, terpenes, and carbohydrates) with reference to salidroside, tyrosol, crenulatin, and rhodionin in the sample. But the exact composition of *R. crenulata* varies according to its geographical source, and the value of utilization of various compounds is also different, such as the phenylpropanoids are thought to be critical for the adaptogenic properties (Ma *et al.*, 2007). It has been also demonstrated to contribute to the sedative-hypnotic, neuroprotective and anti-fatigue effects (Li *et al.*, 2007; Zhang *et al.*, 2007; Ma *et al.*, 2008). Crenulatin (Δ^1-isopentenyl-3-O-β-D-glucopyranoside) is a characteristic hemiterpene compound found only in *R. crenulata* and possesses an anti-apoptosis effect on pulmonary microvascular endothelial cells (Zhang *et al.*, 2004), promoting angiogenesis, anti-anoxia, improving blood circulation, and dissipating blood stasis (Huang *et al.*, 2005). Flavonoids, such as rhodionin (herbacetin 7-O-α-L-rhamnopyranoside) possess anti-thrombotic, antitumor activities (Peng *et al.*, 1996) and can enhance learning and memory (Fan *et al.*, 2001). Carbohydrates have anti-oxidation and anti-radiation capacities (Luo *et al.*, 1994; Zhang, 2008; Li *et al.*, 2017). As we know, in China, people always pay more attention to the genuine medicinal materials. But, there is no definite criterion to choose the plant of which geographical origin produces the genuine medicinal materials and it is not easy to determine the geographical origin with the existing analytical tools as well as through visible and microscopic inspection (Li & Zhang, 2008a; Mou *et al.*, 2016). The compounds salidroside, tyrosol and rhodionin are commonly used as markers to control the quality of *R. crenulata* (Committee of National Pharmacopoeia, 2015; Li & Zhang, 2008b; Li & He, 2016a; Li & He, 2016b). However, it would be advantageous to treat the botanic drugs as a whole rather than rely solely on the commonly used one or two marker compounds. To obtain the profile of all metabolites might be more suitable to evaluate the quality of *R. crenulata*. It is therefore necessary to focus on developing a new comprehensive and effective tool for quality evaluation in herbs. Since ^{1}H NMR can simultaneously detect all proton-bearing compounds in a sample, it has the potential to provide a relatively unbiased fingerprint containing overlapping signals of the majority of the metabolites present in the unpurified solvent extract. Multivariate or pattern recognition techniques such as the well-described principal component (PCA) and partial least squares (PLS) analysis methods are important tools for the analysis of data obtained by NMR. Recently, NMR in combination with PCA/PLS is being increasingly applied to profile metabolites for the quality assessment of crude plant

materials and phytomedicines (Ward *et al*., 2003; Choi *et al*., 2004a, 2004b; Kim *et al*., 2005; Shin *et al*., 2007; Li *et al*., 2016; Li & He, 2017).

In this study, the application of ^{1}H NMR spectroscopy method coupled with multivariate statistical analysis to the profiling of *R. crenulata* samples from different geographical regions is reported. This method gives an overview of the difference between crude drugs of *R. crenulata* originating from different production environments and also could be utilized for the establishment of standardization and quality control procedures for *R. crenulata* based on a variety of metabolites.

Materials and Methods

Plant material: The roots and rhizomes of *R. crenulata* were collected during flowering and fruiting period in trays containing five individual plants from the western Sichuan province plateau areas and Tibet of China. All underground plant material from each tray was combined. The plant materials were air-dried in the dark at ambient temperature for two weeks. Specifications of the samples evaluated in the present study are shown in Table 1. The plants were identified; voucher specimens were deposited in the Herbarium of Pharmacognosy, West China School of Pharmacy, Sichuan University (WCU). The plants with flower, rhizome and root, fruit, and leaf of *R. crenulata* are presented in Fig. 1.

Table 1. *R. crenulata* used in assessment of principal component analysis by ^{1}H NMR spectroscopy.

Sample code	Locality	Date of collection
C0	Wenchuan, Sichuan, China	July, 2015
C1	Pali, Tibet, China	September, 2014
C2	Hongyuan, Sichuan, China	September, 2014
C3	Luding, Sichuan, China	July, 2014
C4	Linzhi, Tibet, China	September, 2013
C5	Heishui, Sichuan, China	August, 2014
C6	Danba, Sichuan, China	August, 2014
C7	Xiaojin, Sichuan, China	July, 2014
C8	Kangding, Sichuan, China	July, 2014
C9	Jiulong, Sichuan, China	August, 2014
C10	Baoxing, Sichuan, China	July, 2014
C11	Songpan, Sichuan, China	September, 2014

Fig. 1. The plants with flower (a), rhizome and root (b), fruit (c), and leaf (d) of *R. crenulata*.

Table 2. ^{1}H-NMR and ^{13}C-NMR data of salidroside (D_2O), tyrosol (CD_3COCD_3), crenulatin (D_2O), and rhodionin (CD_3COCD_3).

No.	Salidroside		Tyrosol		Crenulatin		Rhodionin	
	δ_H (ppm)*J*(Hz)	δ_C(ppm)	δ_H (ppm)*J*(Hz)	δ_C(ppm)	δ_H (ppm)*J*(Hz)	δ_C(ppm)	δ_H (ppm)*J*(Hz)	δ_C(ppm)
1	3.39 t (7.2)	70.1	3.67 t (7.2)	64.1	5.35 d (18.0) 5.28 d (10.8)	117.4		
2	2.92 t (7.2)	35.0	2.70 t (7.2)	39.2	6.04 dd (18.0,10.8)	145.2		147.7
3		128.8		130.8		81.7		136.6
4	7.25 d (8.8)	129.9	7.04 d (8.8)	130.6	1.45 s	28.8		177.0
5	6.90 d (8.4)	115.2	6.74 d (8.4)	115.8	1.42 s	27.7		150.8
6		155.8		156.4			6.73 s	98.7
7	6.90 d (8.4)	115.2	6.74 d (8.4)	115.8				153.0
8	7.25 d (8.8)	129.9	7.04 d (8.8)	130.6				130.7
9								145.1
10								100.6
1′	4.49 d (8.0)	103.0			4.55 d (8.0)	99.8		123.3
2′	3.74 dd (5.6,5.6)	73.6			3.92 d (12.4)	75.7	8.23 d (9.2)	130.7
3′	3.27 dd (8.0,8.0)	76.9			3.72 dd (5.2,5.6)	78.2	7.03 d (8.8)	116.2
4′	3.45 m	70.3			3.26 dd (9.2,8.0)	72.4		160.4
5′	4.13 m	77.1			3.52 m	78.4	7.03 d (8.8)	116.2
6′	3.92 m	61.3			3.42 m	63.5	8.23 d (9.2)	130.7
1″							5.62 d (2.0)	100.6
2″							4.16 dd (2.0,1.6)	71.1
3″							3.96 dd (3.6,5.6)	71.7
4″							3.53 t (9.6)	73.2
5″							3.71 m	70.7
6″							1.24 d (6.4)	18.1

Solvents and chemicals Analytical grade methanol was purchased from Merck Company Inc. (Darmstadt, Germany) for the extraction of herbs. DMSO-d_6 (99.9 Atom % D, cont. 0.05 V/V % TMS) were obtained from ARMAR chemicals Co.. Salidroside, tyrosol, crenulatin, and rhodionin were isolated from *R. crenulata* (Li *et al.*, 2012). In this paper, the complete assignments of ^{1}H and ^{13}C NMR signals for compounds of salidroside, tyrosol, crenulatin, and rhodionin were carried out (Table 2). The structures of compounds were established by direct comparison of their physical and spectroscopic data with those reported in the literature (Li *et al.*, 2012).

Extraction and ^{1}H NMR spectroscopy One gram pulverized sample powder was accurately weighed and transferred into a 25 ml centrifuge tube. Ten ml of methanol was added to the tube, followed by vortexing for 30 sec. and then heating at 50°C in a water bath for 40 min. After cooling, the material was then centrifuged at 3000 rpm for 20 min. The extractions were repeated two times. The supernatants were combined to a 25 ml round-bottomed flask and dried in a rotary vacuum evaporator. The dried sample (20.0mg) was dissolved in 0.4 ml of NMR solvent and used for ^{1}H NMR measurement. ^{1}H NMR and ^{1}H-^{1}H COSY spectra were recorded on a Bruker AVII-600 NMR instrument operating at a proton NMR frequency of 600.13 MHz and acquired under automation at a temperature of 298 K on a Bruker Avance spectrometer. Each ^{1}H NMR spectrum consisted of 64 scans of 64 k data points with a spectral width of 12335.526 Hz using a 90° read-pulse and a water suppression pulse sequence with a relaxation delay of 5.0 s. The spectra were automatically Fourier transformed using an exponential window with a line broadening value of 0.5 Hz, phased and baseline corrected within the automation programme. ^{1}H NMR chemical shifts in the spectra were referenced to TMS at δ 0.00 ppm. The COSY spectrum was acquired with the following parameters: number of experiments 256, number of scans 8, dummy scans 8, and spectral width 7212 Hz in both dimensions. FID resolution was 3.5 Hz in F2 and 28.1 Hz in F1, acquisition time was 142 ms, and relaxation delay was1.0 s. The window function for the COSY spectra was sine-bell (SSB＝0).

Data reduction of the NMR spectra and multivariate data analysis: One dimensional ^{1}H NMR spectra were converted into their first derivative forms and digitised using the software application MestRe-C (version 4.7.0.0, Mestrelab Research, Santiago de Compostela, Spain). Spectral intensities were scaled to TMS and reduced to integrated regions of equal width (0.05 ppm) corresponding to the region of δ 10.0 to δ 0.0 ppm, thus producing 200 discrete bucketed regions. The residual proton signals corresponding to DMSO–d_6 (δ 2.50) and TMS (δ 0.00 ppm) were removed. The digitised data sets could then be imported directly from MestRe-C into SIMCA-P 11.0 (Umetrics, Umea, Sweden) for PCA analysis.

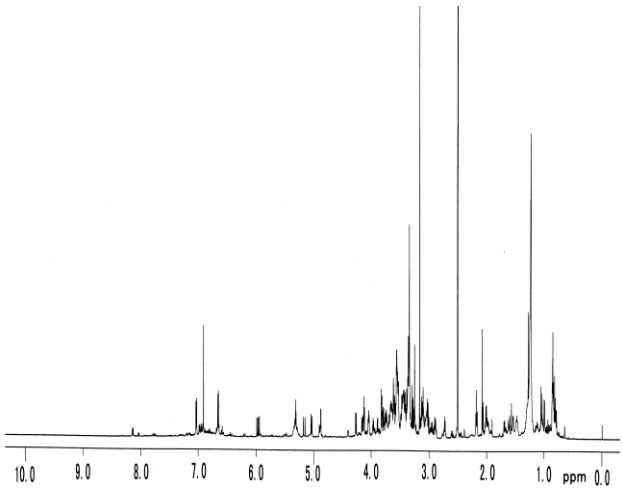

Fig. 2. 600MHz ^{1}H NMR spectrum of methanol extract of *R. crenulata*.

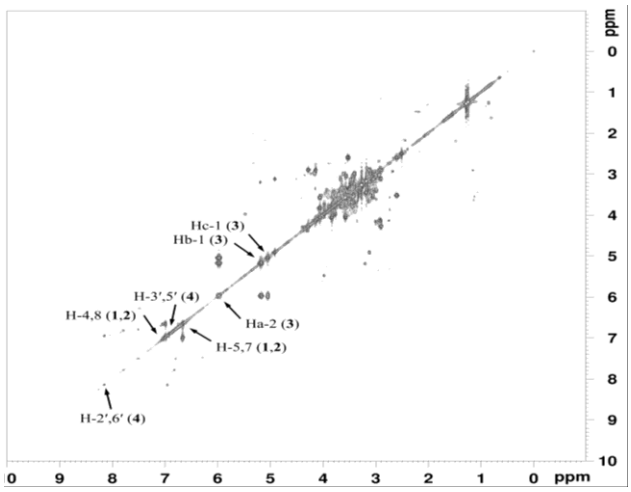

Fig. 3. ^{1}H ^{1}H COSY spectrum of methanol extract of *R. crenulata*.

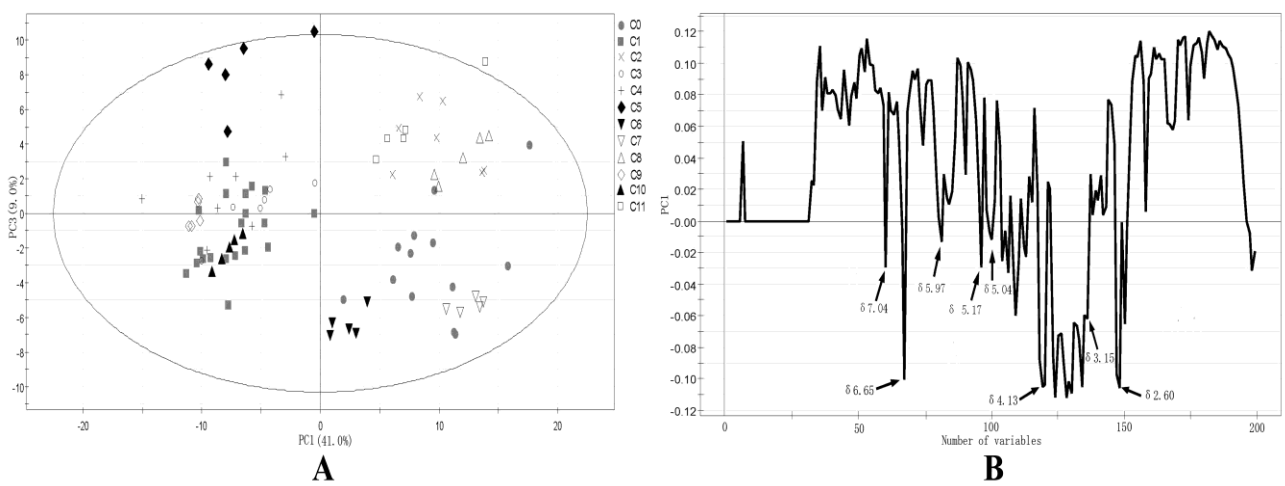

Fig. 4. Score and loading plot generated from PCA of *R. crenulata* from twelve geographical origins. A: scores plot of PC1 vs. PC3. B: loadings plot of PC1.

Results and Discussions

Visual inspection of ^{1}H NMR spectra and assignments of the compounds: For the identification of metabolites such as phenylpropanoids, flavonoids, terpenes, and carbohydrates, methanol extracts were analysed. In general the obtained NMR spectra showed a dominance of signals in the carbohydrate region of the spectrum. In addition to these signals, well-defined signals in both the aromatic and aliphatic regions of the spectra were present (Fig. 2). The signals of the main aromatic compound in the extract were assigned to the compounds of salidroside, tyrosol, and rhodionin based on the comparison of reference compounds. The ^{1}H NMR spectrum was in accordance with phenylpropanoids, showing the characteristic signals due to four aromatic protons at δ 7.04 (2H, d, J = 8.8 Hz) and δ 6.65 (2H, d, J = 8.4 Hz) corresponding to H-4, H-8 and H-5, H-7 of the aromatic ring, and δ 2.60 (2H, t, J = 7.2 Hz) corresponding to H-2 of the compounds of salidroside and tyrosol. The characteristic signals of terpenes, such as crenulatin were well distinguishable in the ^{1}H NMR spectrum of methanol extract. Ha-2 at δ 5.97 (dd, Jab = 18.0 Hz, Jac = 10.8 Hz), Hb-1 at δ 5.17 (d, Jba = 18.0 Hz), Hc-1 at δ 5.04 (d, Jca = 10.8 Hz), C-3 methyl at δ 1.28 (s) and δ 1.23 (s) were observed as major signals in the methanol extract. In addition to these signals of phenylpropanoids and terpenes, those of flavonoids, such as rhodionin were detected as minor signals. The signals of H-2′, H-6′ and H-3′, H-5′ of rhodionin were detected at δ 8.15 (2H, d, J = 9.2 Hz) and δ 6.98 (2H, d, J = 8.8 Hz), respectively. The 2D-COSY spectrum linked the hydrogen atoms in three isolated groups, revealing the homonuclear correlations between H-4, H-8 and H-5, H-7 in the compounds of salidroside and tyrosol, between Ha-2, Hb-1, and Hc-1 in the compound of crenulatin, and between H-2′, H-6′ and H-3′, H-5′ in the compound of rhodionin (Fig. 3). Similarly, the major signals were shown in the anomeric signals of carbohydrates such as δ 4.90 (d, J = 3.7 Hz), and δ 4.27 (d, J = 8.0 Hz). They were assigned to the anomeric hydrogens of α-glucose and β-glucose, respectively. Another anomeric signal obtained from the glucose of the compound of salidroside is also well distinguishable at δ 4.13 (d, J = 8.0 Hz). In the sugar region (δ 3.0-6.0), clear differences among the various geographical regions of *R. crenulata* could be seen. However, it was difficult to identify each peak because a number of signals were overlapping.

For nonbiased interpretation of the results, the samples were analyzed using PCA and PLS methods due to their generally similar metabolomic patterns. Subsequently, further investigations were made to assign the peaks.

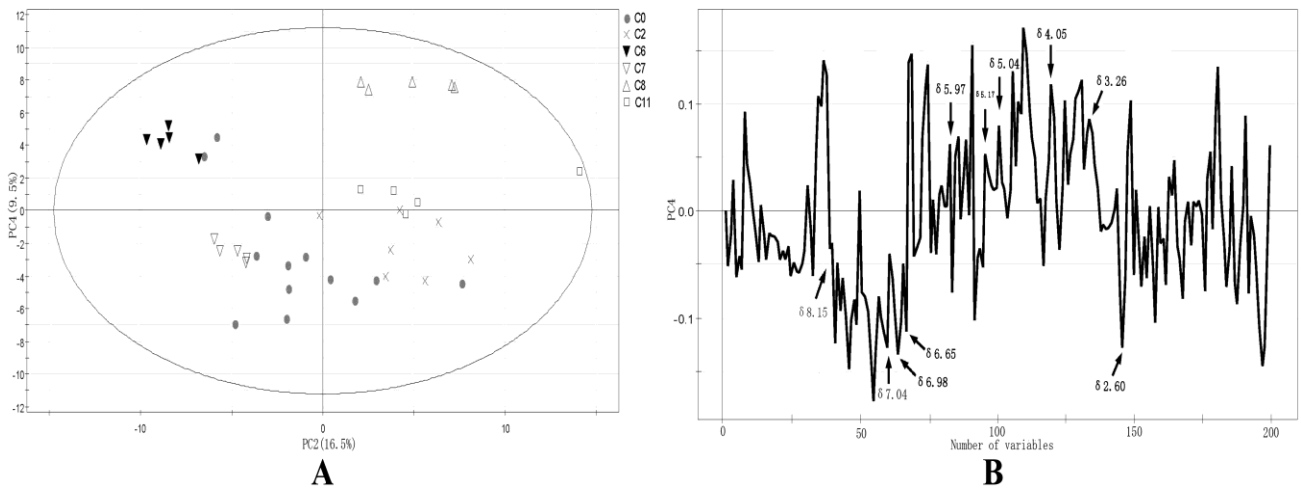

Fig. 5. Score and loading plot generated from PCA of C0, C2, C6, C7, C8, and C11. A: score plot of PC2 vs. PC4. (C0: Wenchuan; C2: Hongyuan; C6: Danba; C7: Xiaojin; C8: Kangding; C11: Songpan) B: loadings plot of PC4.

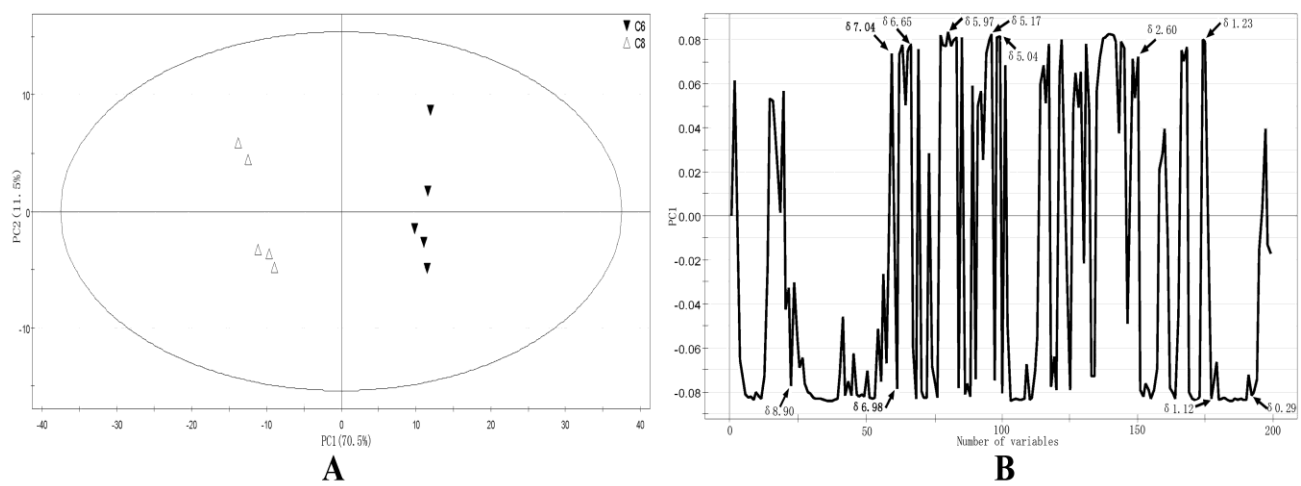

Fig. 6. Score and loading plot generated from PCA of C6 and C8. A: score plot of PC1 vs. PC2. (C6: Danba; C8: Kangding) B: loadings plot of PC1.

Principal component analysis (PCA) of *R. crenulata* data sets according to twelve geographical origins: Principal component analysis (PCA) is an unsupervised clustering method requiring no knowledge of the data set and acts to reduce the dimensionality of multivariate data while preserving most of the variance within it (Eriksson *et al.*, 2001). It enables the easy comparison of plant metabolic profiles. In applying PCA, large differences were observed between the spectra of the methanol fractions of *R. crenulata* samples from the twelve geographical sources, and all the spots in the PCA gathered in the two characteristic groups. As seen in Fig. 4A, there is a clear discrimination between the samples of C1, C3, C4, C5, C9, C10 and C0, C2, C6, C7, C8, C11 of *R. crenulata*. For the data set obtained from the analysis of methanol extract, a seven-component model explained 80.0% of the variance, with the first and third principal components explaining 65.0% of the variability. Among the PCs, the combination of principal component 1 (PC1) and principal component 3 (PC3) can give two well-separated groups for all samples of *R. crenulata* (Fig. 4A). Examination of the scores plot for PC1 vs. PC3 showed that the samples of two groups of *R. crenulata* were clearly separated from each other by the scores of PC1. Examination of the loadings plot of PC1 (Fig. 4B) showed that the first component explained the variance in carbohydrate levels since high negative loadings values were observed for peaks in the carbohydrate region between δ 3.15 and δ 4.13. In addition, the loadings plot of PC1 indicated that the first component explained the variance in phenylpropanoids and terpenes, such as the compounds of salidroside, tyrosol, and crenulatin due to the signals at δ 2.60, 6.65, 7.04 and δ 5.97, 5.17, 5.04 and had an effect on the negative value of PC1. It is evident that six geographical regions of the group of C1, C3, C4, C5, C9, and C10 are separated mainly by virtue of their increase in carbohydrates, phenylpropanoids and terpenes and the decrease in flavonoids from the rest of the group. On the contrary, the amounts of flavonoids are higher in C0, C2, C6, C7, C8, and C11 than those of other samples. For further metabolomic analysis to obtain clear differentiation and determine the nature of chemical compounds in the above two groups, the ^{1}H NMR spectra of the methanol fractions of each group was assessed for PCA.

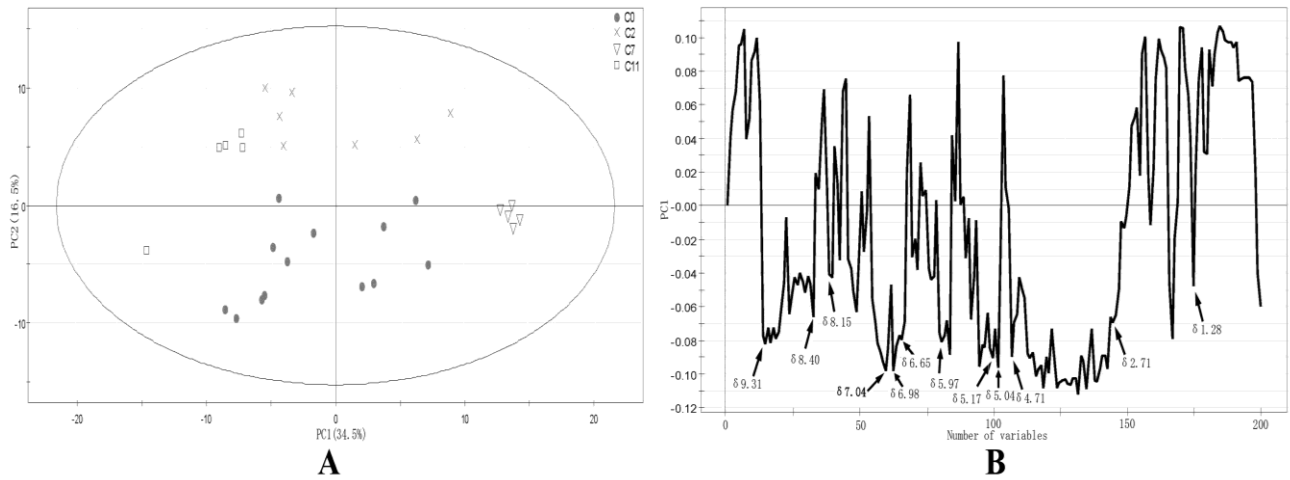

Fig. 7. Score and loading plot generated from PCA of C0, C2, C7 and C11. A: score plot of PC1 vs. PC2. (C0: Wenchuan; C2: Hongyuan; C7: Xiaojin; C11: Songpan) B: loadings plot of PC1.

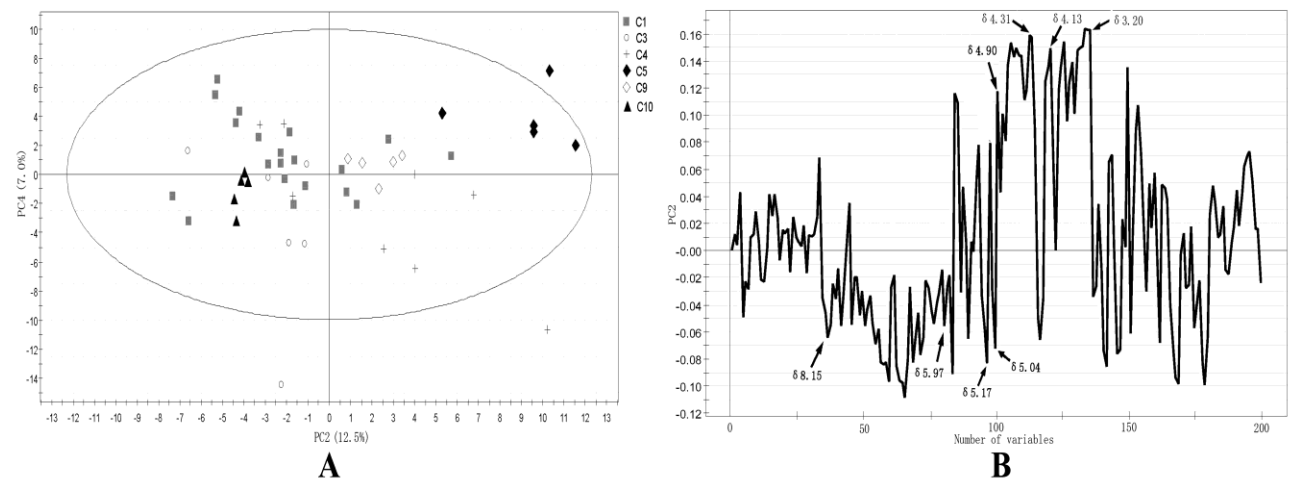

Fig. 8. Score and loading plot generated from PCA of C1, C3, C4, C5, C9, and C10. A: score plot of PC2 vs. PC4. (C1: Pali; C3: Luding; C4: Linzhi; C5: Heishui; C9: Jiulong; C10: Baoxing) B: loadings plot of PC2.

For the data set obtained from the analysis of each methanol extract of the C0, C2, C6, C7, C8, and C11 samples, a seven-component model explained 80.0% of the variance. This separation took place in the second and fourth principal components which cumulatively account for 70.0% of variability and demonstrated a separation of C6 and C8 from the rest of the group (Fig. 5A). The main principal component to differentiate the plants is PC4. Examination of the loadings plot for PC4 (Fig. 5B) shows positive loadings for some signals of δ 5.97, 5.17, 5.04, and δ 3.26-4.05 in the terpenes and carbohydrate regions. Such differences were highlighted by the higher levels of terpenes and carbohydrate, and lower levels of flavonoids and phenylpropanoids in the samples of C6 and C8. In applying PCA to each methanol extract of the C6 and C8 samples, a two-component model explained 82.0% of the variance. C6 and C8 were clearly separated from one another. Examination of the scores plot for PC1 vs. PC2 (Fig. 6A) demonstrated that the separation between the samples of C6 and C8 was easily achieved in the scores of PC1. Examination of the loadings plot for PC1 (Fig. 6B) shows that the samples of C8 separated from those of C6 according to PC1 mainly by virtue of its increase in flavonoids and aliphatic compounds and its decrease in phenylpropanoids and terpenes. In applying PCA to each methanol extract of the C0, C2, C7, and C11 samples, a five-component model explained 78.0% of the variance. Examination of the scores plot for PC1 vs. PC2 (Fig. 7A) demonstrated that the separation between the four samples was easily achieved in the scores of PC1 and PC2. Examination of the loadings plot for PC1 (Fig. 7B) shows that the samples of C7 separated from the C11 according to PC1 is mainly by virtue of its increase in aliphatic compounds and its decrease in phenylpropanoids, flavonoids, terpenes, and carbohydrates. The amounts of these compounds are intermediate in C0 and C2.

For the data set obtained from the analysis of each methanol extract of the C1, C3, C4, C5, C9, and C10 samples, an eight-component model explained 76.0% of the variance. The scores plot for PC2 vs. PC4 (Fig. 8A) is difficult to separate all six sources samples, but examination of the scores plot for PC2 vs. PC4 demonstrated that the separation between the samples of C5, C9 and C3, C10 was easily achieved in the scores of PC2. Examination of the loadings plot for PC2 (Fig. 8B) shows positive loadings mainly for some signals of δ 3.20-4.13 and δ 4.31-4.90 in the carbohydrate regions. The relatively higher PC2 of C5 and

C9 showed that it contained more carbohydrates and less phenylpropanoids, terpenes, and flavonoids. The scores plot of PC2 vs. PC4 can now be summarized to show that the level of carbohydrates in the sample of C5 have the highest amount. In applying PCA to each methanol extract of the C5 and C9 samples, the C5 and C9 samples evaluated are well separated from each other with the scores plot for PC1 vs. PC2 (Fig. 9A). The samples of C5 and C9 were clearly distinguished by PC1. In the loadings plot for PC1 (Fig. 9B), it shows that the samples of C5 are separated from the C9 according to PC1 by virtue of its increase in almost all kinds of compounds. In applying PCA to each methanol extract of the C1, C3 and C10 samples, it is difficult to separate completely all three sources samples for the scores plot for PC1 vs. PC4 (Fig. 10A), but examination of the scores plot for PC1 vs. PC4 and the loadings plot for PC1 (Fig. 10B) also show that the sample of C3 are separated from the C1 and C10 according to PC1 by virtue of its increase in phenylpropanoids and flavonoids and decrease in terpenes.

Partial least squares (PLS) analysis of *R. crenulata* data sets according to the month of collection: In addition to geographical origins, the growing conditions such as the month of collection are also recognized as important factors having effect on the metabolite profiles of *R. crenulata*. The value of the month of collection was used in PLS analysis to determine if these independent variables affect the dependent variables of interest. In applying PLS analysis for the same ^{1}H NMR data set classified according to the month of collection, the samples of twelve geographical origins yielded 5 PLS components to represent 0.651 original data (R2) and a cross-validated R2 (Q2) of 0.465. Examination of the scores plot for PLS1 vs. PLS2 (Fig. 11A) demonstrated that the separation between the samples of C1, C4, C5, C6, C9, C10 and C0, C2, C7, C8, C11 was easily achieved in the scores of PLS1. The spectral domains explaining this separation were identified as resonances of phenylpropanoids (7.04, 6.65, 2.60 ppm), terpenes (5.97, 5.17, 5.04 ppm) and carbohydrates (3.20-4.05 ppm) in the positive side of PLS1 axis, and flavonoids (8.15, 6.98 ppm) in the negative side of PLS1 axis (Fig. 11B). These suggested that the samples of C1, C4, C5, C6, C9, and C10 presented higher relative amounts of phenylpropanoids, terpenes and carbohydrates and relatively lower amounts of flavonoids than those of the samples of C0, C2, C7, C8, and C11.

It was found that the chemical composition of the cohort of *R. crenulata* is diverse and mostly mapped well classified according to the geographical origins of the samples studied. Because the chemical compositions in *R. crenulata*, with various biological activities, are highly variable according to its geographical source, the quality control of this complex material and the choice of the genuine medicinal materials should be determined according to clinic application. The results showed that the contents of phenylpropanoids, producing the effects of sedative-hypnotic and anti-fatigue, in samples from Luding, Pali, and Baoxing are higher than those of other samples, and that in samples from Kangding is the lowest. Terpenes, which possess properties of anti-apoptosis, promoting angiogenesis, anti-anoxia, in samples from Pali, Baoxing, and Luding containing the higher levels, and that in samples from Xiaojin is the lowest. Carbohydrates with anti-radiation and anti-oxidation capacities were higher in the *R. crenulata* from Heishui, Jiulong, Pali, Baoxing, Linzhi and Luding than in the other samples, and that in samples from Xiaojin was the lowest. The result indicated that the geographical origins samples of Luding, Pali, and Baoxing were of excellent quality and evidently curative effects in anti-fatigue, sedative-hypnotic, anti-anoxia, and anti-radiation, etc. However, the contents of flavonoids which possess anti-thrombotic, antitumor, and enhancing learning and memory activities in samples from Songpan, Wenchuan, and Hongyuan are higher than those of other samples, and that in samples from Jiulong is the lowest, indicating that the geographical origins samples of Songpan, Wenchuan, and Hongyuan have the excellent quality and evidently curative effects in anti-thrombotic, enhancing learning and memory, etc. In addition, the quality of *R. crenulata* is closely related to the concentrations of their chemical constituents. The "gold standard" in the *R. crenulata* from Pali in Tibet could serve as a "control". Fold changes in relative concentration of the major metabolites of interest contributed to the differentiation of *R. crenulata* from different geographical origins were determined and shown in Table 3.

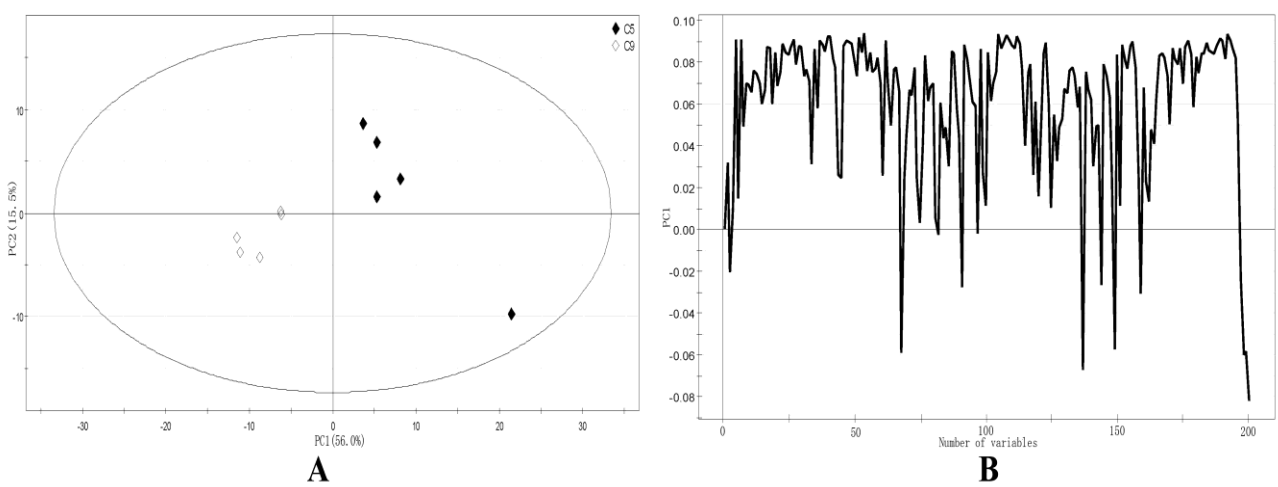

Fig. 9. Score and loading plot generated from PCA of C5 and C9. A: score plot of PC1 vs. PC2. (C5: Heishui; C9: Jiulong) B: loadings plot of PC1.

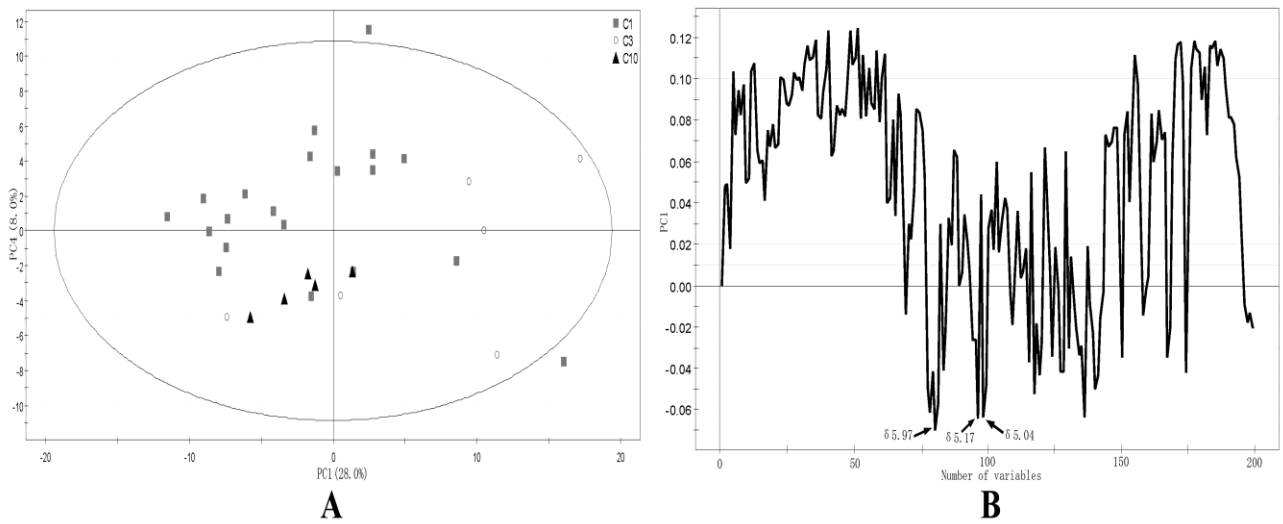

Fig. 10. Score and loading plot generated from PCA of C1, C3, and C10. A: score plot of PC1 vs. PC4. (C1: Pali; C3: Luding; C10: Baoxing) B: loadings plot of PC1.

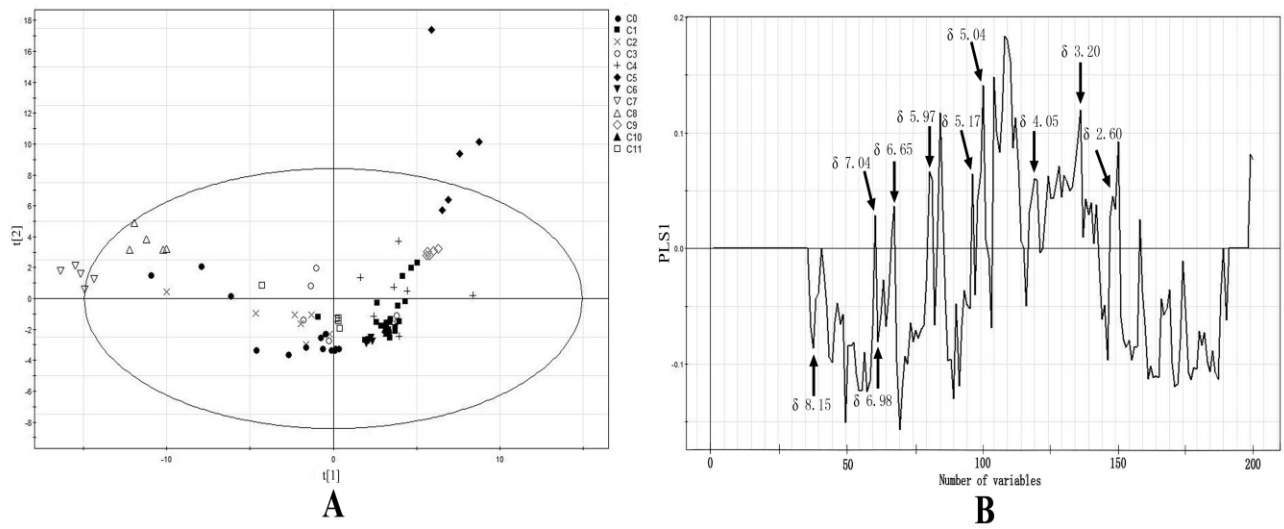

Fig. 11. Score and loading plot generated from PLS of *R. crenulata* from twelve geographical origins classified according to the month of collection. A: scores plot of PLS1 vs. PLS2. B: loadings plot of PLS1.

Table 3. Fold changes in relative concentration of the major metabolites of interest.

Sample code	Salidroside + Tyrosol (δ 7.04)	Crenulatin (δ 5.97)	Rhodionin (δ 8.15)	α-Glucose (δ 4.90)	β-Glucose (δ 4.27)
C0	0.324 ± 0.143	0.446 ± 0.254	0.609 ± 0.355	0.322 ± 0.168	0.269 ± 0.105
C1	1.000 ± 0.506	2.057 ± 0.975	0.082 ± 0.021	1.067 ± 0.590	0.530 ± 0.260
C2	0.887 ± 0.344	0.828 ± 0.404	0.086 ± 0.028	0.426 ± 0.273	0.232 ± 0.082
C3	1.024 ± 0.556	0.325 ± 0.169	0.080 ± 0.020	0.357 ± 0.176	0.295 ± 0.141
C4	0.586 ± 0.281	1.398 ± 0.645	0.074 ± 0.021	0.362 ± 0.236	0.309 ± 0.137
C5	0.307 ± 0.137	1.747 ± 0.906	0.078 ± 0.017	0.567 ± 0.331	0.370 ± 0.220
C6	0.301 ± 0.105	0.883 ± 0.402	0.023 ± 0.010	0.355 ± 0.159	0.234 ± 0.071
C7	0.514 ± 0.292	0.321 ± 0.135	0.099 ± 0.036	0.051 ± 0.015	0.299 ± 0.095
C8	0.249 ± 0.119	0.835 ± 0.337	0.024 ± 0.011	0.548 ± 0.316	0.761 ± 0.227
C9	0.316 ± 0.120	1.110 ± 0.561	0.020 ± 0.007	0.398 ± 0.207	0.195 ± 0.069
C10	0.955 ± 0.411	3.258 ± 1.385	0.116 ± 0.053	0.373 ± 0.209	0.283 ± 0.104
C11	0.950 ± 0.397	0.570 ± 0.252	0.238 ± 0.094	0.407 ± 0.225	0.318 ± 0.101

Conclusion

In this study, the method using ^{1}H NMR and multivariate data analysis is potentially useful as a tool in the accurate evaluation of different sources of *R. crenulata* based on metabolic profiles. PCA and PLS highlighted genuine differences between geographical regions with loadings plots giving clues as to the nature of these differences. Comparison of the spectra run under identical conditions, the score and loading plot show that phenylpropanoids, flavonoids, terpenes and carbohydrates are important metabolites to differentiate *R. crenulata* from various geographical regions. Compared with the currently used quality assessment protocol, this method permits a much more reasonable and efficient manner to ensure the efficacy and safety, and may also be used in the future as a first screen to rapidly define similarities between different batches of *R. crenulata* to ensure batch-to-batch *R. crenulata* uniformity. This approach also laid the foundation for the selection of optimal geographical origins and cultivation locality of *R. crenulata* with excellent quality and evidently curative effects according to clinic application. The proposed method is rapid and reproducible and could be readily utilized as a new quality control technique for *R. crenulata* and *R. crenulata* derived herbal products.

Acknowledgments

This study was supported by research grants from the Applied Basic Research Project of Sichuan Science and Technology Department (No. 2016JY0247) and Technology Huimin Technology Research and Development Project of Chengdu Science and Technology Bureau (No. 2016-HM01-00339-SF).

References

Choi, H.K., Y.H. Choi, M. Verberne, A.W.M. Lefeber, C. Erkelens and R. Verpoorte. 2004b. Metabolic fingerprinting of wild type and transgenic tobacco plants by ^{1}H NMR and multivariate analysis technique. *Phytochem*., 65: 857-864.

Choi, Y.H., H.K. Kim, A. Hazekamp, C. Erkelens, A.W.M. Lefeber and R. Verpoorte. 2004a. Metabolomic differentiation of *Cannabis sativa* cultivars using ^{1}H NMR spectroscopy and principal component analysis. *J. Nat. Prod*., 67: 953-957.

Committee of National Pharmacopoeia. 2015. *Pharmacopoeia of the People's Republic of China*. China Medical Science Press, Beijing.

Eriksson, L., E. Johansson, N. Kettaneh-Wold and S. Wold. 2001. *Multi- and Megavariate Data Analysis*. Umetrics Academy, Umeå, Sweden.

Fan, W.Z., Y. Tezuka, K.M. Ni and S. Kadota. 2001. Prolyl endopeptidase inhibitors from the underground part of *Rhodiola sachalinensis*. *Chem. Pharm. Bull.*, 49: 396-401.

Huang, H.Q., K.J. Cheng, G.L. Liang and C.Q. Hu. 2005. Separation, synthesis and content analysis of crenulatin. *Nat. Prod. Res. Dev.*, 17: 468-470.

Kim, H.K., Y.H. Choi, C. Erkelens, A.W.M. Lefeber and R. Verpoorte. 2005. Metabolic fingerprinting of *Ephedra* species using ^{1}H NMR spectroscopy and principal component analysis. *Chem. Pharm. Bull.*, 53: 105-109.

Li, T. and H. Zhang. 2008a. Application of microscopy in authentication of traditional Tibetan medicinal plants of five *Rhodiola* (Crassulaceae) alpine species by comparative anatomy and micromorphology. *Microsc. Res. Tech.*, 71: 448-459.

Li, T. and H. Zhang. 2008b. Identification and comparative determination of rhodionin in traditional Tibetan medicinal plants of fourteen *Rhodiola* species by high-performance liquid chromatography-photodiode array detection and electrospray ionization-mass spectrometry. *Chem. Pharm. Bull.*, 56: 807-814.

Li, T. and X. He. 2016a. Quantitative analysis of salidroside and *p*-tyrosol in the traditional Tibetan medicine *Rhodiola crenulata* by fourier transform near-Infrared spectroscopy. *Chem. Pharm. Bull*., 64: 289-296.

Li, T. and X. He. 2016b. Studies on two economically and medicinally important plants, *Rhodiola crenulata* and *Rhodiola fastigiata* of Tibet and Sichuan province, China. *Pak. J. Bot.*, 48: 2031-2038.

Li, T. and X. He. 2017. Classification of *Rhodiola crenulata* and *Rhodiola fastigiata* based on ^{1}H-NMR fingerprint combined with chemical pattern recognition technique. *Lishizhen Medicine and Materia Medica Research*, 28: 888-891.

Li, T., Z.L. Ge and X. He. 2017. Comparative study and determination polysaccharide content of thirteen medicinal plants of *Rhodiola* from the western Sichuan province plateau. *West China J. Pharm. Sci.*, 32: 529-530.

Li, T., Z.L. Ge and H. Zhang. 2012. Study on the chemical constituents of *Rhodiola crenulata*. *West China J. Pharm. Sci.*, 27: 367-370.

Li, T.L., G.H. Xu, L.L. Wu and C.Y. Sun. 2007. Pharmacological studies on the sedative and hypnotic effect of salidroside from the Chinese medicinal plant *Rhodiola sachalinensis*. *Phytomedicine*, 14: 601-604.

Li, X., S. Jiang and C. Man. 2016. Metabolomic analysis of female and male plants of *Pistacia chinensis* Bunge. *Pak. J. Bot.*, 48: 1971-1977.

Luo, C.H., Y. Gao, Z.H. Wang, X.Z. Liu and Z.L. Ge. 1994. Study on the antiradiation effect of *Rhodiola crenulata* polysaccharide. *Chin. J. Radiol. Med. Prot.*, 14: 340-341.

Ma, L., D.L. Cai, H.X. Li, B.D. Tong, L.H. Song and Y. Wang. 2008. Anti-fatigue effects of salidroside in mice. *J. Med. Univ. PLA.*, 23: 88-93.

Ma, L.Q., B.Y. Liu, D.Y. Gao, X.B. Pang, S.Y. Lü, H.S. Yu, H. Wang, F. Yan, Z.Q. Li, Y.F. Li and H.C. Ye. 2007. Molecular cloning and overexpression of a novel UDP-glucosyltransferase elevating salidroside levels in *Rhodiola sachalinensis*. *Plant Cell Rep.*, 26: 989-999.

Mou, F.J., K. Ma, S.Z. Ma, S.Z. Duan and Y.G. Li. 2016. Morphological diversity of leaf and its geographic differentiation of *Citrus cavaleriei* from Yunnan. *Pak. J. Bot.*, 48: 2343-2350.

Peng, J.P., T. Narui, H. Suzuki, R. Ishii, H. Abuki and T. Okuyama. 1996. Anti-blood coagulation and cytotoxic effects of compounds from Chinese plants used for thrombosis-like diseases. *Natural Medicines*., 50: 358-362.

Shin, Y.S., K.H. Bang, D.S. In, O.T. Kim, D.Y. Hyun, I.O. Ahn, B.C. Ku, S.W. Kim, N.S. Seong, S.W. Cha, D. Lee and H.K. Choi. 2007. Fingerprinting analysis of fresh ginseng roots of different ages using ^{1}H NMR spectroscopy and principal components analysis. *Arch. Pharm. Res.*, 30: 1625-1628.

Ward, J.L., C. Harris, J. Lewis and M.H. Beale. 2003. Assessment of ^{1}H NMR spectroscopy and multivariate analysis as a technique for metabolite fingerprinting of *Arabidopsis thaliana*. *Phytochem.*, 62: 949-957.

Yang, Y.C., T.N. He, S.L. Lu, R.F. Hung and Z.X. Wang. 1991. *Zang Yao Zhi*. Qinghai People's Publishing House, Xining.

Zhang, G.P., H.M. Jin, W.J. Wang and F. Le. 2004. Effect of crenulatin on apoptosis of rats pulmonary microvascular endothelial cells in vitro. *J. Chin. Microcirc.*, 8: 272-273.

Zhang, L., H.X. Yu, Y. Sun, X.F. Lin, B. Chen, C. Tan, G.X. Cao and Z.W. Wang. 2007. Protective effects of salidroside on hydrogen peroxide-induced apoptosis in SH-SY5Y human neuroblastoma cells. *Eur. J. Pharmacol.*, 564: 18-25.

Zhang, S.M.. 2008. Study on the extraction of polysaccharide from *Rhodiola crenulata* by alkali method and its antioxidation. *J. Anhui Agri. Sci.*, 36: 7741-7742.

(Received for publication 11 December 2016)